• Basic Research •

In vitro adherence of conjunctival bacteria to different oculoplastic materials

Alvaro Toribio[1], Honorina Martínez-Blanco[2], Leandro Rodríguez-Aparicio[2], Miguel Á. Ferrero[2], Teresa Marrodán[3], Isabel Fernández-Natal[3]

[1]Department of Ophthalmology, University Hospital of León, León 24071, Spain
[2]Department of Molecular Biology, University of León, León 24071, Spain
[3]Department of Clinical Microbiology, University Hospital of León, León 24071, Spain
Correspondence to: Alvaro Toribio. Department of Ophthalmology, University Hospital of Leon. Altos de Nava s/n, Leon 24071, Spain. draltor@gmail.com
Received: 2018-05-25 Accepted: 2018-09-18

Abstract

• AIM: To investigate the resistance to bacterial adhesion of materials used in oculoplastic surgery, particularly materials used in the manufacture of orbital implants.

• METHODS: Seven organisms of conjunctival flora (two strains of *Staphylococcus epidermidis* and one strain each of *Staphylococcus aureus, Staphylococcus hominis, Corynebacterium amycolatum, Acinetobacter calcoaceticus,* and *Serratia marcescens*) were selected. A lactic acid bacterium (*Lactobacillus rhamnosus*) was also included as positive control because of its well-known adhesion ability. Eight materials used to make oculoplastic prostheses were selected (glass, steel, polytetrafluoroethylene, polymethylmethacrylate, silicone from orbital implants, commercial silicone, porous polyethylene, and semi-smooth polyethylene). Materials surfaces and biofilms developed by strains were observed by scanning electron microscopy. Kinetics of growth and adhesion of bacterial strains were determined by spectrophotometry. Each strain was incubated in contact with plates of the different materials. After growth, attached bacteria were re-suspended and colony-forming units (CFUs) were counted. The number of CFUs per square millimetre of material was statistically analyzed.

• RESULTS: A mature biofilm was observed in studied strains except *Staphylococcus hominis*, which simply produced a microcolony. Materials showed a smooth surface on the microbial scale, although steel exhibited 1.0-μm-diameter grooves. Most organisms showed significant differences in adhesion according to the material. There were also significant differences in the total number of CFUs per square millimetre from each material (*P*=0.044). CFU counts were significantly higher in porous polyethylene than in silicone from orbital implants (*P*=0.038).

• CONCLUSION: Silicone orbital implants can resist microbial colonization better than porous polyethylene implants.

• KEYWORDS: conjunctival flora; microbial adhesion; biofilm; orbital implant; oculoplastic prosthesis
DOI:10.18240/ijo.2018.12.03

Citation: Toribio A, Martínez-Blanco H, Rodríguez-Aparicio L, Ferrero MÁ, Marrodán T, Fernández-Natal I. *In vitro* adherence of conjunctival bacteria to different oculoplastic materials. *Int J Ophthalmol* 2018;11(12):1895-1901

INTRODUCTION

One of the main complications associated with the use of medical devices is their microbial colonization. This process depends on the characteristics of both the prosthetic material and the colonizing microorganism[1]. In the field of ophthalmology, responsible microorganisms are usually those living in the conjunctiva[2]. The conjunctival flora comprises a diverse group of species, among which coagulase-negative staphylococci and coryneform bacteria stand out[3]. The adhesion and biofilm development by microorganisms of the conjunctival flora have been widely valued in intraocular lenses[4-7]. However, the materials used in oculoplastic surgery have been much less explored. Although bacterial biofilms have been demonstrated on symptomatic periocular prostheses[8], there are no studies comparing *in vitro* resistance to bacterial adhesion of these materials.

The purpose of this study is to analyze resistance to microbial adhesion of several materials used in oculoplastic surgery to select the most appropriate material for situations with high risk of infection.

MATERIALS AND METHODS

Bacterial Strains Eight bacterial strains were used to assess their adhesion to different oculoplastic materials. Four strains were purchased from the Spanish Type Culture Collection (CECT): *Staphylococcus epidermidis* CECT 231 (*S. epidermidis*), *Acinetobacter calcoaceticus* CECT 441 (*A. calcoaceticus*),

Corynebacterium amycolatum CECT 4163 (*C. amycolatum*), and *Lactobacillus rhamnosus* CECT 278 (*L. rhamnosus*). The other four strains [*S. epidermidis*, *Staphylococcus aureus* (*S. aureus*), *Staphylococcus hominis* (*S. hominis*) and a non-pigmented *Serratia marcescens* (*S. marcescens*)] were obtained from the conjunctival swab of healthy eyes from patients who participated in a previous study. This study was approved by the institutional review board of our hospital. The techniques used to collect the data conformed to the tenets of the Declaration of Helsinki. Written informed consent was obtained from all study patients before participation. These wild strains were identified in the clinical microbiology laboratory of our hospital. The strain of *S. epidermidis* isolated from a patient was called *S. epidermidis* wild-type (WT), to differentiate it from the strain *S. epidermidis* CECT 231.

Strains of CECT were initially grown in the specific recommended media, while wild strains were seeded on plates with tryptone soy agar (TSA). Afterwards, the adequate growth of all strains in TSA medium at 37℃ was verified.

Dynamics of Growth and Adhesion Each strain was initially cultured on a TSA plate for 24h at 37℃. These cells were then seeded in a slant tube with TSA, which was cultured again under same conditions. Cells from the slant tube were then re-suspended in 5 mL phosphate buffered saline (PBS). The dilution was adjusted until it reached a concentration of 1.0 optical density measured at 540 nm (OD_{540}). One milliliter of this dilution was inoculated in a 250-mL flask with 50 mL tryptone soy broth (TSB) medium. The flask was incubated at 37℃ in a rotary shaker at 200 rpm. The growth curve of each strain was obtained by measuring the OD_{540}.

Bacterial adhesion was quantified in 96-well polystyrene microtiter plates. Cells cultured in TSB under agitation were collected at the end of the exponential growth phase, according to the previously calculated growth curve. Each strain was diluted to get a bacterial suspension of 1.0 OD_{540}. Twenty microliters of this suspension was added into a microtiter well with 180 μL TSB. Each strain was incubated in six replicate wells at 37℃ without agitation.

Adhered cells were quantified by the crystal violet method following the modifications described by Shimizu *et al*[6]. However, we used crystal violet at 0.1% concentration and color readings were made at 570 nm. The kinetic curve of adhesion from each strain was performed by measuring the microtiter plates at 4, 6, 8, 12, 24, 36 and 48h of incubation.

Biofilm Formation Ability The ability of strains to develop a biofilm was determined using scanning electron microscopy (SEM). Biofilm maturity was established in three grades: irreversible attachment (monolayer microbial growth); microcolony (multilayer bacterial growth); and mature biofilm (multilayer growth with abundant extracellular matrix and channel formation at the biofilm base)[1].

The bacteria were incubated in contact with polytetrafluoroethylene (Teflon) plates. Strains were first cultured in TSB for 12h under agitation at 37℃. In a 24-well polystyrene plate, a sterile Teflon sheet was deposited at the bottom of a well. Next, 1.9 mL TSB and 100 μL bacterial suspension 1.0 OD_{540} were added. The plate was incubated without agitation at 37℃. Strains were incubated for 24 to 48h, according to the kinetic curves of adhesion to polystyrene. Finally, the Teflon plates were extracted and the formed biofilms were observed using a SEM (JSM-6480 LV, JEOL, Tokyo, Japan).

Oculoplastic Materials The selected materials have been widely used in oculoplastic surgery[9-10]: glass, steel, Teflon, polymethylmethacrylate (PMMA), silicone, high density porous polyethylene (HDPP), and semi-smooth polyethylene (SSP; a sheet of non-porous polyethylene with one surface covered of HDPP)[11].

Samples of the materials were obtained from different sources: glass was obtained by cutting optical microscopy slides, stainless steel and Teflon coupons were acquired from Alfa Aesar (Heysham, UK), PMMA from acrylic resin of ocular prostheses (provided with the appropriate form and measurements by the ocularist M.P.), silicone samples were obtained from orbital implants (FCI, Paris, France) and commercial stoppers (Saint-Gobain Verneret, Charny, France), and HDPP and SSP by cutting sheets of orbital reconstruction (Porex Surgical, Newnan, GA, USA).

Plate-shaped samples of approximately 10×10×1 mm^3 were obtained from each material. The exact area of the contact surface exposed to microorganisms was measured in mm^2 for each plate.

Bacterial Attachment to the Materials The materials were cleaned by sonication for 30min in PBS at 45 kHz. Subsequently, they were sterilized using 70% ethanol for 10min[12]. The surfaces of the 8 selected materials were examined by SEM to find out the level of superficial irregularities.

The bacterial adhesion experiment was developed in 24-well polystyrene microtiter plates. All wells were engaged in every plate because each of the 8 materials was analyzed in three replicative wells. Thus, one microtiter plate was used for the adhesion study of each strain. Based on their growth curves, bacteria were previously cultured in TSB under agitation at 37℃ for 12h (20h in the case of *A. calcoaceticus*) and diluted to 1.0 OD_{540}. Therefore, each well was filled with a cleaned and sterile material sample, 1.9 mL TSB, and 100 μL dilution of the corresponding strain. The plate was incubated without agitation at 37℃ for 12h.

To evaluate the bacterial attachment, each material sample was extracted and carefully washed with 2 mL sterile distilled water to remove non-attached cells. Then, the sample was placed in a 50-mL tube with 1 mL PBS. The attached cells

Table 1 Evolution of bacterial adhesion to polystyrene

Bacterial strains	Time of incubation (h)						
	4	6	8	12	24	36	48
S. epidermidis CECT	0.30±0.05	0.43±0.03	0.46±0.08	0.43±0.07	0.30±0.03	0.25±0.03	0.22±0.03
S. epidermidis WT	0.17±0.05	0.27±0.03	0.32±0.04	0.35±0.03	0.34±0.05	0.26±0.03	0.18±0.03
S. aureus	0.28±0.06	0.38±0.02	0.45±0.04	0.56±0.04	0.59±0.03	0.34±0.04	0.23±0.15
S. hominis	0.04±0.01	0.16±0.06	0.18±0.03	0.19±0.03	0.18±0.04	0.17±0.02	0.13±0.01
C. amycolatum	0.10±0.03	0.12±0.01	0.13±0.03	0.13±0.01	0.13±0.03	0.12±0.08	0.09±0.07
A. calcoaceticus	0.05±0.01	0.06±0.02	0.07±0.02	0.09±0.02	0.09±0.02	0.07±0.00	0.06±0.04
S. marcescens	0.71±0.04	1.03±0.07	1.18±0.13	1.23±0.06	1.06±0.13	0.55±0.08	0.42±0.04
L. rhamnosus	0.02±0.02	0.12±0.01	0.21±0.04	0.25±0.06	0.20±0.01	0.19±0.05	0.13±0.01

Data are mean±SD of units of OD at 540 nm. CECT: Spanish type culture collection; WT: Wild-type.

were re-suspended by agitation in vortex at 1500 rpm for 10s and seeded in plates with TSA. After growing for 24h at 37℃, colony-forming units (CFUs) were counted.

The CFUs obtained were adjusted per unit of material surface and were transformed into a decimal logarithm, following the method used by other authors[5-6]. Therefore, the unit of measurement of bacterial adhesion to a material was expressed as $\log_{10}$ CFUs/mm^2.

Statistical Analysis The adhesion results were measured in units of OD (adhesion curves to polystyrene) and CFUs/mm^2 (bacterial adhesion), so they were presented as the mean±standard deviation (SD).

The CFUs recovered from each material were analyzed using the non-parametric Kruskal-Wallis test with the Dunn-Bonferroni post hoc method to pairwise comparison. A *P* value of less than 0.05 was considered statistically significant. Statistical analysis was conducted using SPSS for Windows version 22.0 (SPSS Inc., Chicago, IL, USA). Charts were drawn with GraphPad Prism 5 for Windows (GraphPad Software Inc., La Jolla, CA, USA).

RESULTS

Dynamics of Growth, Adhesion and Biofilm Development

The growth curves of the selected strains are shown in Figure 1. *S. aureus* and *S. marcescens* showed the highest levels of cell multiplication, while *A. calcoaceticus* and lactic acid bacteria *L. rhamnosus* showed the lowest growth. Most of the conjunctival strains had reached the exponential growth phase at 12h of culture under agitation, beginning their cell death phase at 20h.

However, *A. calcoaceticus* reached the exponential growth phase at 20h of culture. Based on these outcomes, subsequent experiments were conducted with cultures of the strains in TSB under agitation for 20h for *A. calcoaceticus* and for 12h for the remaining microorganisms.

Regarding the bacterial adhesion to polystyrene, *S. aureus* and especially *S. marcescens* showed more adhered cells, although the two strains of *S. epidermidis* also exhibited high levels of adhesion (Table 1). In contrast, *C. amycolatum* and *A. calcoaceticus* revealed a poor adhesion to polystyrene. All

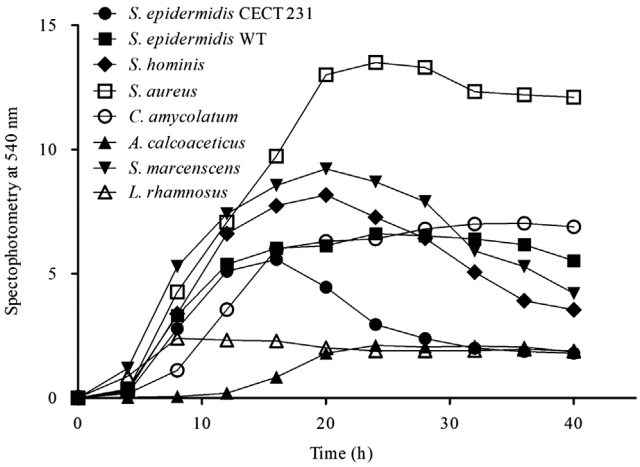

Figure 1 Growth curves of the selected bacterial strains CECT: Spanish type culture collection; WT: Wild-type.

strains had the highest level of attached cells at approximately 12h of incubation (Table 1). Therefore, the incubation time of the strains with the different samples of the materials was for 12h for all bacteria.

The SEM images of the attached bacteria determined that all the studied strains except *S. hominis* developed a mature biofilm (Figure 2). The cells of *S. hominis* remained grouped in a microcolony with a minimal production of extracellular matrix. Conversely, the biofilms formed by the other studied strains showed a profuse extracellular matrix with micro-channels.

Bacterial Adhesion to Selected Materials Surfaces of the selected materials were generally flat on a microbial scale (Figure 3). Glass showed one of the smoothest surfaces, despite presenting some small irregularities. Teflon, PMMA, HDPP, and SSP exhibited a relatively smooth surface similar to "cracked earth," while silicones had a granular appearance. The steel sample was the only one that displayed grooves of about 0.5 μm, although they were poorly interconnected.

Bacterial adhesion differed significantly according to the material among *S. epidermidis* CECT, *C. amycolatum*, *A. calcoaceticus*, *S. marcescens* and *L. rhamnosus* (Table 2). Except for *S. marcescens*, a pairwise comparison test could not determine differences in adhesion between materials.

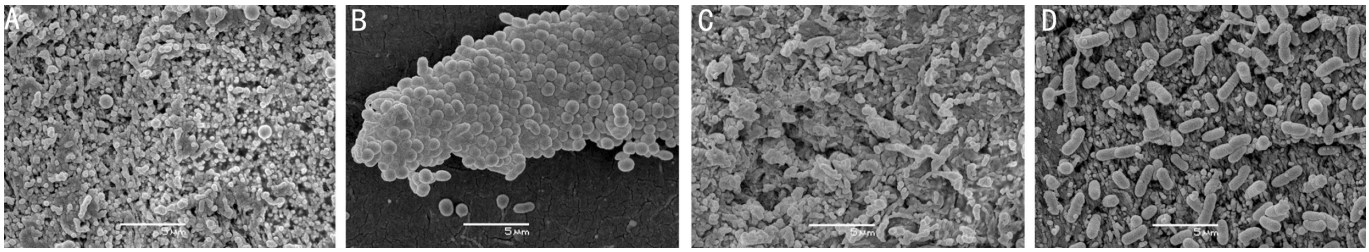

Figure 2 Scanning electron microscopy of biofilms formed on polystyrene plates All images were taken at 5000 magnifications. Except for *S. hominis*, the studied strains developed mature biofilms with abundant extracellular matrix and channels at their base. A: *S. epidermidis* CECT at 24h of incubation; B: *S. hominis* at 48h; C: *C. amycolatum* at 48h; D: *S. marcescens* at 24h.

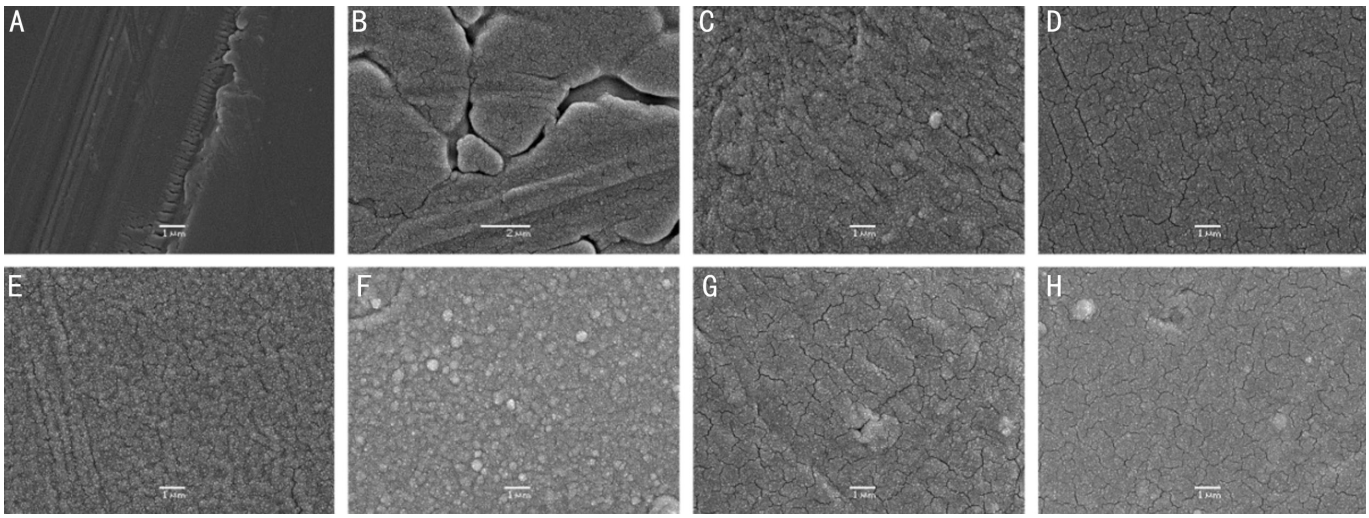

Figure 3 Scanning electron microscopy of the selected materials All images were taken at 10 000 magnifications. Steel was the only material with grooves of a size similar to the bacterial diameter. A: Glass; B: Steel; C: Teflon; D: Polymethylmethacrylate; E: Orbital implant silicone; F: Commercial silicone; G: High density porous polyethylene; H: Semi-smooth polyethylene.

Table 2 Quantification of adhered bacteria to the materials

Bacterial strains	Glass	Steel	PMMA	Teflon	OI silicone	Comercial silicone	SSP	HDPP	P^a
S. epidermidis CECT	6.42±0.57	5.95±0.12	6.03±0.23	5.94±0.21	5.41±0.26	5.50±0.05	6.86±0.61	6.82±0.17	0.010
S. epidermidis WT	6.87±0.44	7.02±0.59	7.03±0.94	7.69±0.38	7.15±0.84	6.55±0.12	7.28±0.21	7.24±0.36	0.450
S. aureus	6.99±0.36	7.37±0.10	7.05±0.49	7.48±0.02	6.56±0.32	6.56±1.15	7.42±0.15	7.13±0.11	0.066
S. hominis	6.85±0.19	6.79±0.41	6.93±0.45	6.86±0.09	5.27±0.23	6.51±0.63	6.71±0.60	7.64±0.64	0.135
C. amycolatum	3.68±0.16	3.73±0.11	3.99±0.11	3.99±0.13	4.02±0.33	4.37±0.18	3.67±0.03	4.52±0.17	0.010
A. calcoaceticus	4.71±0.10	4.53±0.13	4.92±0.21	4.94±0.13	5.00±0.22	5.07±0.31	4.72±0.15	5.11±0.05	0.046
S. marcescens	5.76±0.05	5.81±0.12	5.90±0.03	5.85±0.18	5.23±0.26	5.93±0.44	6.34±0.50	6.65±0.37	0.032
L. rhamnosus	7.12±0.34	7.32±0.28	7.20±0.27	7.41±0.56	5.62±0.93	6.25±0.19	6.94±0.45	7.33±0.13	0.045

Bacterial counting in $\log_{10}$CFU/mm^2±SD. CECT: Spanish type culture collection; WT: Wild-type; $\log_{10}$CFU/mm^2: Base-10 logarithm of colony forming units per squared millimeter of material surface; PMMA: Polymethylmethacrylate; OI silicone: Orbital implant silicone; SSP: Semi-smooth polyethylene; HDPP: High density porous polyethylene. [a]Kruskal-Wallis test.

S. marcescens exhibited a preferential adhesion to HDPP compared with silicone from orbital implant (P=0.018).

HDPP had the most CFUs per mm^2 with *S. hominis*, *C. amycolatum*, *A. calcoaceticus* and *S. marcescens*. Moreover, HDPP was the second material with more CFUs per mm^2 of *S. epidermidis* CECT and *L. rhamnosus*. However, silicone from orbital implants had the least adhesion of *S. epidermidis* CECT, *S. aureus*, *S. hominis*, *S. marcescens* and *L. rhamnosus*.

Regardless of the strain type, the total number of CFUs per mm^2 recovered from each material (Figure 4) showed significant differences in Kruskal-Wallis tests (P=0.044). After performing the pairwise comparison analysis, a higher adhesion to HDPP was observed with respect to silicone from orbital implants (P=0.038).

DISCUSSION

In this study, we compared the bacterial adhesion with different oculoplastic materials and found a statistically significantly higher CFU count in the HDPP compared with silicone from

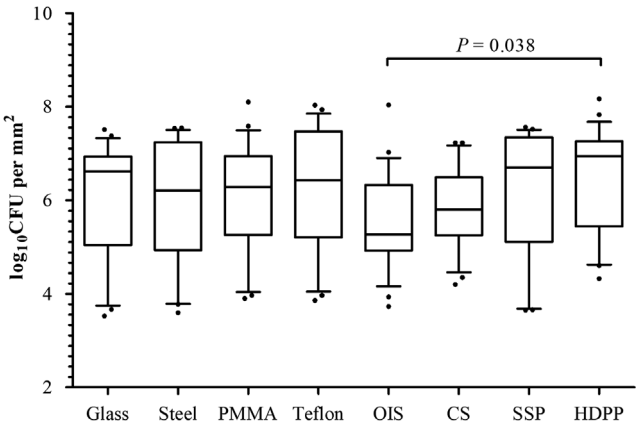

Figure 4 Box-plot of CFU recovered from each material Data are in decimal logarithm of CFU/mm^2 of material. The top and bottom of the box show the third and first quartiles, respectively, with the median shown as the band inside the box. The top and bottom error bar show the 90 and 10 percentile, respectively. Outliers are shown as black circles. PMMA: Polymethylmethacrylate; OIS: Orbital implant silicone; CS: Commercial silicone; SSP: Semi-smooth polyethylene; HDPP: High density porous polyethylene.

orbital implants. Because microbial adhesion to an abiotic surface depends on both the organism and the material[13], we also studied the kinetic characteristics of the selected strains and the roughness of the materials.

Bacterial strains used in this study are representative of the conjunctival flora[3,14-15], except for *L. rhamnosus*. We selected three strains of coagulase-negative *Staphylococcus* (*S. epidermidis* CECT 231, *S. epidermidis* WT, and *S. hominis*) and a coryneform bacteria, *C. amycolatum*. These strains are considered saprophytic species. As pathogenic microorganisms, we used *S. aureus* and the Gram-negative coccobacillus *S. marcescens* (with high degree of pathogenicity)[16] and *A. calcoaceticus* (with low pathogenicity)[17]. Although lactic acid bacteria are not present in the conjunctival flora, *Lactobacillus rhamnosus* was selected as adhesion control strain for its well-known attachment ability[18].

The growth and adhesion kinetics of the selected strains correlated with their clinical and epidemiological characteristics. *S. aureus* and *S. marcescens* exhibited the highest growth levels (Figure 1) and adhesion to polystyrene (Table 1). These data agree with pathogenic bacteria because both growth and adhesion ability favor microbial survival[19]. Conversely, *A. calcoaceticus* showed low growth levels (Figure 1) and adhesion to polystyrene (Table 1) and other materials (Table 2). Although it can produce nosocomial infections and keratitis in contact lens wearers[17,20], this Gram-negative species is considered a human commensal of relatively low virulence that colonizes rather than infects[17]. The two strains of *S. epidermidis* exhibited an intermediate level of adhesion to polystyrene (Table 1), clearly superior to the control strain *L. rhamnosus*. Although *S. epidermidis* is referred to as the typical saprophyte species, it is the first etiological agent of corneal ulcers[21] and endophthalmitis[22]. *S. hominis* and *C. amycolatum* showed relatively high growth but poor attachment to polystyrene (Table 1). Krolasik *et al*[23] determined that *S. hominis* produces a small amount of extracellular matrix, according to its low pathogenic capacity[24]. In the present study, this was confirmed by SEM because *S. hominis* was the only strain that produced a microcolony and not a mature biofilm (Figure 2). Conversely, *C. amycolatum* developed a dense biofilm. Although this species is regarded as a normal inhabitant of the skin, *C. amycolatum* is increasingly associated with infections of medical devices such as joint prostheses[25] or orbital implants[26]. Therefore, although there were differences in the degree of growth and adhesion, all the selected strains had the ability to adhere to abiotic surfaces.

The key finding of this study is that bacteria adhered more intensely to HDPP than to silicone from orbital implants (Figure 4). This can be explained by differences in the material surface, because porosity and roughness are crucial parameters that influence the adhesion of bacteria[27]. Pores in a material mainly cause a surface enlargement depending on the pore size and the degree of interconnection[13]. Conversely, roughness can be defined as a pattern of fine-spaced irregularities[28] with a magnitude similar to the bacterial size. Although surface irregularities (such as cracks, furrows, or grooves) also slightly increase the total available surface, they favor microbial adhesion as increasing the direct contact between the material and microorganism walls[28]. SEM images of the selected materials revealed no cracks on the surface similar in size to the bacterial diameter (from 0.5 to 1 μm), except for steel (Figure 3). These 1-μm grooves in the stainless steel are common in this material[23]. However, the other observed samples, even the porous ones, were smooth on a microbial scale (Figure 3).

Therefore, we consider the increase in the surface area to be the main factor of the higher bacterial attachment observed for HDPP. Porous materials such as HDPP have a greater available contact area, which can be over 700% larger than an ideal plane[13]. Braem *et al*[13] noticed a significant increase in bacterial adhesion over a titanium sheet with pores of only 50 μm compared with a smooth-surface titanium. HDPP implants have 100- to 500-μm pores[29], which translates to an important increase of the available surface and consequently means greater microbial attachment. However, it should also be noted that differences in adhesion were significant only with respect to silicone and not against other non-porous materials such as glass, Teflon, or PMMA (Figure 4). In this sense, Mazoteras and Casaroli-Marano[7] also demonstrated a lower bacterial adhesion to silicone intraocular lenses with respect to PMMA lenses, especially when they measured the number of CFUs after 72h of incubation.

Based on these outcomes, we advise oculoplastic surgeons to consider using silicone orbital implants in those cases with a high probability of infection, such as replacing exposed orbital implants or in eviscerations due to endophthalmitis. Bee *et al*[30] described a high risk for primary implant exposure after enucleation and evisceration in infected eyes when patients have a preoperative leukocyte count above 9500 cells/L. The surgical trauma from explanting an infected implant may cause fibrosis and harm the extraocular muscles[31]. Moreover, a two-stage operation may be needed to manage extensive orbital implant exposure during implant removal and replacement[32]. These situations should make us think about the importance of using orbital implants manufactured with materials resistant to the microbial adhesion. Although porous orbital implants are the most frequently used nowadays[33-34], non-porous implants do not show differences in motility or in the exposure rate[9]. Really, the only advantage of porous orbital implants is that they can be covered with an autologous graft if an exposure occurs.

Limitations of our study included some narrow circumstances with the materials. HDPP was the only porous material assessed. In addition, sheets of the materials were employed instead of complete orbital implants. Our bacterial adhesion technique required materials to have a plate-shape small enough to be inserted into each of 24 wells of the microtiter plate (approximately $10\times10\times1$ mm^3). Therefore, some samples were obtained from original materials (glass, steel, PMMA, and Teflon) since the prosthetic products could not be trimmed in sheets with the required dimensions. Nevertheless, orbital implant silicone, HDPP, and SSP samples were obtained directly from final oculoplastic prostheses. We continue to evaluate the bacterial adhesion in other porous materials commonly employed in the manufacture of orbital implants, such as natural hydroxyapatite, synthetic hydroxyapatite, and alumina. Additionally, clinical trials are necessary to compare the rate of exposures in anophthalmic patients with HDPP implants with that in patients with silicone implants.

In conclusion, this study shows that bacterial adhesion to porous polyethylene is greater than to silicone. Although no significant differences were found among non-porous materials, the results suggest that silicone could be more resistant to bacterial attachment than other smooth materials. Although further clinical studies are necessary to confirm this laboratory research, silicone orbital implants may be a good option in anophthalmic patients with a high risk of primary implant exposure.

ACKNOWLEDGEMENTS

This study has been communicated at the Spanish Society of Orbital and Oculoplastic Surgery Annual Meeting, 2016 and awarded with the prize for the best communication of the meeting.

Foundations: Supported by the Dirección General de Investigación (SAF 2015-64306-R); the Junta de Castilla y León, Spain (LE283U14).

Conflicts of Interest: Toribio A, None; **Martínez-Blanco H,** None; **Rodríguez-Aparicio L,** None; **Ferrero MÁ,** None; **Marrodán T,** None; **Fernández-Natal I,** None.

REFERENCES

1 Costerton JW, Stewart PS, Greenberg EP. Bacterial biofilms: a common cause of persistent infections. *Science* 1999;284(5418):1318-1322.

2 Speaker MG, Milch FA, Shah MK, Eisner W, Kreiswirth BN. Role of external bacterial flora in the pathogenesis of acute postoperative endophthalmitis. *Ophthalmology* 1991;98(5):639-650.

3 Suto C, Morinaga M, Yagi T, Tsuji C, Toshida H. Conjunctival sac bacterial flora isolated prior to cataract surgery. *Infect Drug Resist* 2012;5:37-41.

4 Baillif S, Hartmann D, Freney J, Kodjikian L. Intraocular lens and bacterial adhesion: influence of the environmental factors, the characteristics of the bacteria, and the target material surface. *J Fr Ophtalmol* 2010;33(3):210-221.

5 Kodjikian L, Burillon C, Chanloy C, Bostvironnois V, Pellon G, Mari E, Freney J, Roger T. In vivo study of bacterial adhesion to five types of intraocular lenses. *Invest Ophthalmol Vis Sci* 2002;43(12):3717-3721.

6 Shimizu K, Kobayakawa S, Tsuji A, Tochikubo T. Biofilm formation on hydrophilic intraocular lens material. *Curr Eye Res* 2006;31(12):989-997.

7 Mazoteras P, Casaroli-Marano RP. In vitro biofilm distribution on the intraocular lens surface of different biomaterials. *J Cataract Refract Surg* 2015;41(9):1980-1988.

8 Samimi DB, Bielory BP, Miller D, Johnson TE. Microbiologic trends and biofilm growth on explanted periorbital biomaterials: a 30-year review. *Ophthalmic Plast Reconstr Surg* 2013;29(5):376-381.

9 Baino F, Perero S, Ferraris S, Miola M, Balagna C, Verné E, Vitale-Brovarone C, Coggiola A, Dolcino D, Ferraris M. Biomaterials for orbital implants and ocular prostheses: overview and future prospects. *Acta Biomater* 2014;10(3):1064-1087.

10 Karesh JW. Biomaterials in ophthalmic plastic and reconstructive surgery. *Curr Opin Ophthalmol* 1998;9(5):66-74.

11 Kwon SI, Kim YJ. Upper eyelid retraction after periorbital trauma. *Korean J Ophthalmol* 2008;22(4):255-258.

12 Kim H, Ryu JH, Beuchat LR. Attachment of and biofilm formation by *Enterobacter sakazakii* on stainless steel and enteral feeding tubes. *Appl Environ Microbiol* 2006;72(9):5846-5856.

13 Braem A, Van Mellaert L, Mattheys T, Hofmans D, de Waelheyns E, Geris L, Anné J, Schrooten J, Vleugels J. Staphylococcal biofilm growth on smooth and porous titanium coatings for biomedical applications. *J Biomed Mater Res A* 2014;102(1):215-224.

14 Gunduz A, Gunduz A, Cumurcu T, Seyrek A. Conjunctival flora in Behcet patients. *Can J Ophthalmol* 2008;43(4):476-479.

15 Toribio A, Marrodan T, Fernandez-Natal I, Martínez-Blanco H, Rodríguez-Aparicio L, Ferrero MÁ. Study of conjunctival flora in anophthalmic patients: influence on the comfort of the socket. *Graefes Arch Clin Exp Ophthalmol* 2017;255(8):1669-1679.

16 Samonis G, Vouloumanou EK, Christofaki M, Dimopoulou D, Maraki S, Triantafyllou E, Kofteridis DP, Falagas ME. Serratia infections in a general hospital: characteristics and outcomes. *Eur J Clin Microbiol Infect Dis* 2011;30(5):653-660.

17 Marcovich A, Levartovsky S. Acinetobacter exposure keratitis. *Br J Ophthalmol* 1994;78(6):489-490.

18 Mailander-Sanchez D, Braunsdorf C, Grumaz C, *et al*. Antifungal defense of probiotic *Lactobacillus rhamnosus* GG is mediated by blocking adhesion and nutrient depletion. *PLoS One* 2017;12:e0184438.

19 Foster TJ, Geoghegan JA, Ganesh VK, Hook M. Adhesion, invasion and evasion: the many functions of the surface proteins of *Staphylococcus aureus*. *Nat Rev Microbiol* 2014;12(1):49-62.

20 Murray CK, Hospenthal DR. Treatment of multidrug resistant Acinetobacter. *Curr Opin Infect Dis* 2005;18(6):502-506.

21 Schaefer F, Bruttin O, Zografos L, Guex-Crosier Y. Bacterial keratitis: a prospective clinical and microbiological study. *Br J Ophthalmol* 2001;85(7):842-847.

22 Gentile RC, Shukla S, Shah M, Ritterband DC, Engelbert M, Davis A, Hu DN. Microbiological spectrum and antibiotic sensitivity in endophthalmitis: a 25-year review. *Ophthalmology* 2014;121(8):1634-1642.

23 Krolasik J, Zakowska Z, Krepska M, Klimek L. Resistance of bacterial biofilms formed on stainless steel surface to disinfecting agent. *Pol J Microbiol* 2010;59(4):281-287.

24 Sychev YV, Vemulakonda GA. Chronic *Staphylococcus hominis* endophthalmitis following injury with a retained intraocular foreign body. *Eye (Lond)* 2014;28(12):1517.

25 Cazanave C, Greenwood-Quaintance KE, Hanssen AD, Patel R. Corynebacterium prosthetic joint infection. *J Clin Microbiol* 2012;50(5):1518-1523.

26 Toribio JA, Marrodan T, Fernandez-Natal I. Orbital implant infection by *Corynebacterium amycolatum*. *Orbit* 2017;36(5):344-346.

27 Dhom J, Bloes DA, Peschel A, Hofmann UK. Bacterial adhesion to suture material in a contaminated wound model: Comparison of monofilament, braided, and barbed sutures. *J Orthop Res* 2017;35(4):925-933.

28 Taylor RL, Verran J, Lees GC, Ward AJ. The influence of substratum topography on bacterial adhesion to polymethyl methacrylate. *J Mater Sci Mater Med* 1998;9(1):17-22.

29 Mawn LA, Jordan DR, Gilberg S. Scanning electron microscopic examination of porous orbital implants. *Can J Ophthalmol* 1998;33(4):203-209.

30 Bee YS, Lin MC, Sheu SJ, Ng JD. Elevated white blood cell count may predict risk of orbital implant exposure. *Can J Ophthalmol* 2014;49(1):45-49.

31 Toft PB, Rasmussen ML, Prause JU. One-stage explant-implant procedure of exposed porous orbital implants. *Acta Ophthalmol* 2012;90(3):210-214.

32 Kim HK, La TY. Treatment of intractable orbital implant exposure with a large conjunctival defect by secondary insertion of the implant after preceding dermis fat graft. *Int J Ophthalmol* 2013;6(2):193-197.

33 Su GW, Yen MT. Current trends in managing the anophthalmic socket after primary enucleation and evisceration. *Ophthal Plast Reconstr Surg* 2004;20(4):274-280.

34 Viswanathan P, Sagoo MS, Olver JM. UK national survey of enucleation, evisceration and orbital implant trends. *Br J Ophthalmol* 2007;91(5):616-619.